MAE 263F Final

Ursa Z., University of California Los Angeles

***Abstract*—Granular jamming is a simple and powerful mechanism for achieving variable stiffness in soft robots. In this work, I develop a discrete element / discrete-elastic-rod (DER-style) simulation of a soft robotic segment consisting of a viscoelastic core surrounded by a granular sleeve. Both the core and sleeve are modeled with bonded and contact particles, respectively, so that the entire structure is represented in a unified particle framework. A dimensionless vacuum parameter scales grain–grain and grain–core contact stiffness to represent unjammed, fully jammed, and spatially varying jamming states. I perform two-dimensional (2-D) and three-dimensional (3-D) dynamic simulations under gravity and tendon loading, compute curvature and elastic energy along the core, and run preliminary sweeps over the jamming level. In addition, I implement a quasi-static Newton solver for the core with jamming-dependent stiffness. The results show that, in 2-D, jamming produces a strong reduction in tip deflection and local curvature, while in 3-D with the current parameters jamming mainly affects transient dynamics and curvature distribution rather than the final tip sag. The bond-energy and curvature fields reveal how half-jammed configurations shift bending into softer regions. The Newton solver is structurally in place but does not yet converge from a straight initial configuration, highlighting directions for future work.**

I. Introduction

Soft robots can safely interact with humans and uncertain environments due to their inherent compliance, but this same compliance limits load-carrying capability and positional accuracy. Variable-stiffness mechanisms, such as granular, layer, and chain jamming, provide a promising way to switch between compliant and rigid modes on demand. In granular jamming, a flexible membrane is filled with grains; when no vacuum is applied, the grains can rearrange and the structure behaves like a fluid-like bag, but when vacuum is applied, increased normal forces and friction between grains make the assembly stiff and solid-like. This principle has been used to build universal jamming grippers and variable-stiffness manipulators.

Most modeling efforts for jamming mechanisms either use continuum finite element methods, material point methods such as ChainQueen for soft robots, or treat the granular pack separately from the soft body. However, the discrete element method (DEM), originally developed by Cundall and Strack for granular assemblies, naturally captures grain-scale contact, friction, and rearrangements. Integrating a DEM-style sleeve with a bonded-particle representation of the soft core offers a unified framework for exploring how micro-scale parameters influence macro-scale stiffness in jamming-based soft robots.

To address these questions, I developed a 2-D prototype and a more realistic 3-D dynamic model, perform parametric studies over jamming profiles, and implement a quasi-static Newton solver for the core with jamming-dependent stiffness.

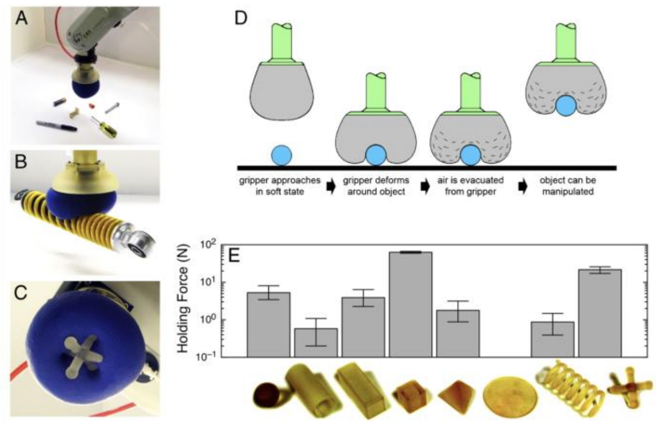

Jamming-based grippers for picking up a wide range of objects without the need for active feedback. (A) Attached to a fixed-base robot arm. (B) Picking up a shock absorber coil. (C) View from the underside. (D) Schematic of operation. (E) Holding force F_h for several three-dimensional-printed test shapes (the diameter of the sphere shown on the very left, 2R = 25.4 mm, can be used for size comparison). The thin disk could not be picked up at all.

II. Background

Granular jamming has been widely explored for universal grippers, variable-stiffness manipulators, and medical devices. Brown *et al.* introduced the “universal robotic gripper” based on a membrane filled with granular material that transitions from unjammed to jammed under vacuum, enabling secure grasp of diverse objects. Subsequent work refined the gripper design and investigated commercialization. Jamming has also been integrated into variable-stiffness arms and chain-like structures for soft robots, demonstrating large stiffness variations through granular, layer, and hybrid jamming. Recent reviews summarize the design and control of granular jamming devices for soft robotics and medical applications.

The discrete element method (DEM), or distinct element method, models granular materials as collections of discrete particles interacting through contact forces and friction. The original work of Cundall and Strack formulated DEM with explicit time integration, contact detection, and contact laws for spheres and discs. DEM has since been applied to soils, powders, and rock mechanics, and is a natural foundation for simulating jammed granular sleeves.

For continuum soft-robot modeling, recent work such as ChainQueen uses the moving least squares material point method (MLS-MPM) to simulate deformable objects, including soft robots with contact, and provides differentiability for co-design and control. My work does not aim to compete with such sophisticated continuum simulators but instead explores a simpler DEM-style model that treats both the soft core and granular sleeve as particles, enabling intuitive exploration of micro-scale jamming behavior.

III. PHYSICAL MODEL

A. Geometry and Materials

The system consists of a single soft segment of length $L_{\text{core}} = 0.15$ m and radius $r_{\text{core}} = 5$ mm. The core cross-sectional area is $A_{\text{core}} = \pi r_{\text{core}}^2$. The core material has density ρcore≈900kg/m^3 and Young's modulus $E_{\text{core}} \approx 50$ kPa, typical of soft polymers.
Around the core, a granular sleeve is formed by spherical beads of radius $r_{\text{bead}} = 4$ mm and density ρbead ≈ 1500kg/m^3.
Beads are randomly distributed in an annular region with inner radius Rinner=rcore+gap, and outer radius Router =rcore+3rbead, where the gap is chosen to avoid initial interpenetration. For the 3-D simulations, each core node has six beads around it, leading to $N_{\text{core}} = 21$ core particles and $N_{\text{sleeve}} = 126$ beads. Gravity acts on all particles with acceleration $\mathbf{g} = (0, -9.81, 0)^{\top}$. A planar ground at $y = y_{\text{ground}} = -0.03$ m provides environmental contact.

B. Jamming Parameter

Granular jamming is modeled via a dimensionless vacuum level $v \in [0,1]$. The level $v = 0$ corresponds to the unjammed state, while $v = 1$ represents full jamming. The vacuum level scales the normal contact stiffness: kcontact(v)=kbase (1+γvac * v) where kbase is a baseline contact stiffness and γvac is a gain factor (e.g., γvac =20). In uniform jamming experiments, a single v is used for all contacts. In the half-jammed case, contacts involving beads in the distal half of the rod use a higher localv, while the proximal half remains soft.

IV. DISCRETE ELEMENT FORMULATION

A. Core: Bonded-Particle Chain

The core is discretized as a one-dimensional chain of Ncore particles with positions xi in Rd and velocities vi. The reference spacing is Δx= Lcore/(Ncore−1).

Neighboring particles i and j=i+1 are connected by Kelvin–Voigt bonds with axial stiffness kbond= Ecore Acore/Δx, and dashpot coefficient cbond. For each bond, the current separation and extension are ℓij=‖xj−xi‖, eij=ℓij−Δx, with unit direction $\mathbf{e}_{ij} = (\mathbf{x}_j - \mathbf{x}_i)/\ell_{ij}$. The relative velocity along the bond is e˙ij=(vj−vi)·eij. The bond force is Fij =(kbondeij+cbonde˙ij)eij, applied as -Fij to node i and +Fij to node j. This bonded-particle model approximates a discrete elastic rod in axial stretching and provides bending stiffness through the geometry of the chain.

B. Contact Model for Sleeve and Core

All particles (core and sleeve) participate in contact interactions. For a pair of particles i and j with radii r_i and r_j, positions $\mathbf{x}_i$, $\mathbf{x}_j$, and velocities $\mathbf{v}_i$, $\mathbf{v}_j$, the relative vector is $\mathbf{d} = \mathbf{x}_j - \mathbf{x}_i$ with magnitude $d = \| \mathbf{d} \|$. The overlap and normal direction are δn=ri+rj−d, n=d/d. Contact occurs when $\delta_n > 0$. The normal relative velocity is δ˙n=(vj−vi)·n. The normal contact force is Fn=kcontact(vij)δn+ccontactδ˙n, where $k_{\text{contact}}(v_{ij})$ depends on the local jamming level and c_{contact} is a dashpot coefficient. The corresponding vector force is $\mathbf{F}_n = F_n \mathbf{n}$. To model friction, the tangential relative velocity is $\mathbf{v}_t = (\mathbf{v}_j - \mathbf{v}_i) - \dot{\delta}_n \mathbf{n}$. A viscous tangential force is applied: $\mathbf{F}_t^{\text{visc}} = -c_t \mathbf{v}_t$, and its magnitude is limited by a Coulomb friction coefficient μ: ‖Ft‖=min(‖Ftvisc‖, μ|Fn|), Ft=Ftvisc·min(1, μ|Fn|/‖Ftvisc‖). The total contact force on particle i is $-(\mathbf{F}_n + \mathbf{F}_t)$, and on j it is the opposite.

C. External Loads and Boundary Conditions

The equations of motion for particle i are mix¨i=Fibond +Ficontact+mig+Figround+Fitendon, where m_i is the particle mass.

1. Boundary conditions
   a. Clamped base: **:** The first core node (index 0) is clamped: x0(t)=xbase,v0(t)=0. In the code, this is enforced at every step by resetting position and velocity of node 0 to their initial values.
   b. Free tip with tendon actuation: The last core node (index $N_{\text{core}} - 1$) is free and experiences a prescribed tendon force. In the simplest configuration, a constant downward force F_{tip} in the $-y$ direction is applied: FNcore−1tendon=(0, −Ftip , 0)T
   c. Ground Plane: A planar ground at $y = y_{\text{ground}}$ prevents particles from falling indefinitely. If particle i has vertical position $y_i < y_{\text{ground}}$, a penalty force is applied: Fi,yground=kground(yground−yi)−cgroundy˙i, representing a unilateral contact with damping.

D. Time integration

Dynamic simulations use **semi-implicit (symplectic) Euler** with time step Δt:

1. Compute all forces at time t^n based on $\mathbf{x}^n$ and $\mathbf{v}^n$.
2. Update velocities: $\mathbf{v}_i^{n+1} = \mathbf{v}_i^n + \Delta t\, \mathbf{a}_i^n$, where $\mathbf{a}_i^n = \mathbf{F}_i^n / m_i$.
3. Update positions: $\mathbf{x}_i^{n+1} = \mathbf{x}_i^n + \Delta t\, \mathbf{v}_i^{n+1}$.
4. Re-impose the clamped boundary at the base node.

This explicit scheme is simple and compatible with DEM's contact-by-contact updates.

V. NUMERICAL EXPERIMENTS

A. 2-D Dynamic Benchmark

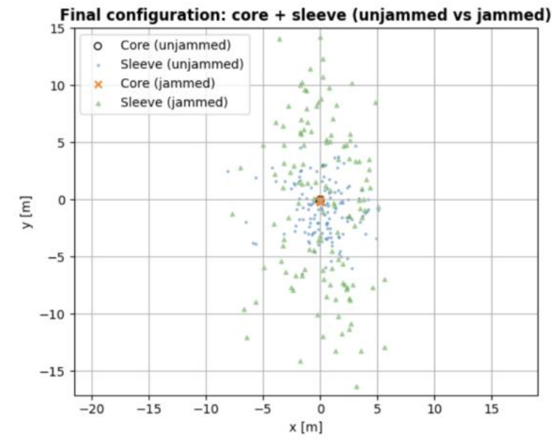

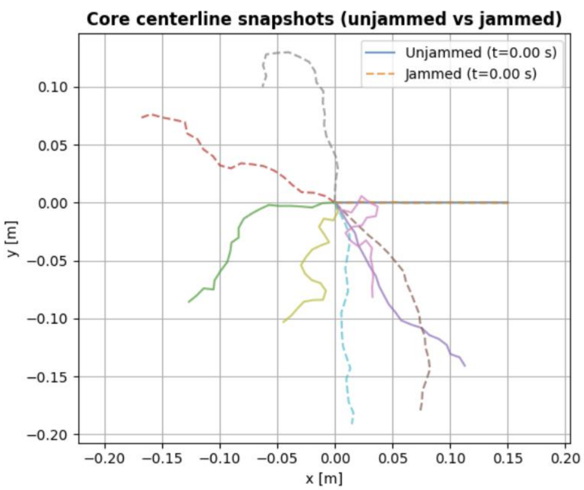

As a first step, I implemented the model in 2-D (x–y plane) with core particles constrained to move in the plane and beads distributed in a ring around each core node. Two simulations are run:

Unjammed: vacuum level $v = 0$.

Fully jammed: vacuum level $v = 1$. Both simulations are run for $T = 0.4$ s with $\Delta t = 10^{-4}$ s, under gravity and a constant downward tip force.

In 2-D, the unjammed rod exhibits large downward bending: the tip reaches approximately -0.2 m under the combined effect of gravity and tendon loading, with multiple oscillations before settling. In contrast, the jammed rod shows a significantly reduced deflection and a different oscillation pattern. Core centerline snapshots over time clearly show that the unjammed configuration develops sharp bends, while the jammed configuration remains closer to a slightly curved cantilever. These results qualitatively reproduce experimental observations that granular jamming can dramatically increase stiffness and reduce deflection in soft structures.

B. 3-D Dynamic Simulations

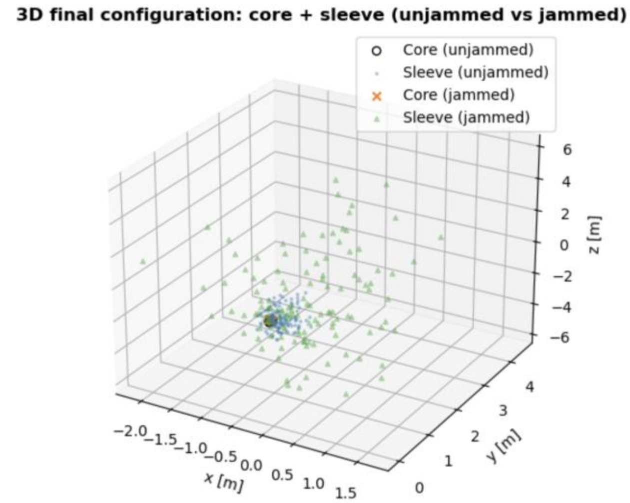

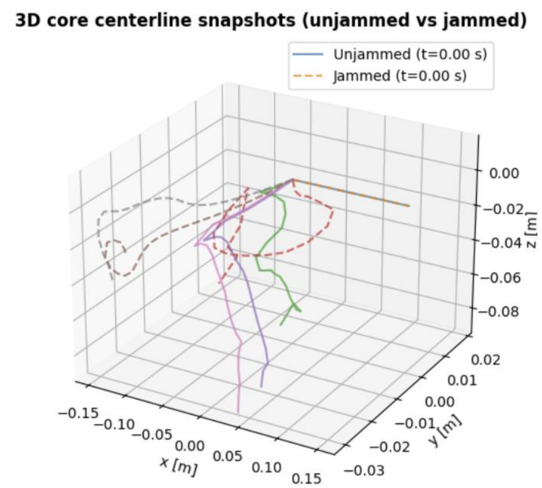

For the 3-D model, three cases are considered:

1. Unjammed: uniform vacuum level $v = 0$.
2. Fully jammed: uniform vacuum level $v = 1$.
3. Half-jammed: proximal half soft, distal half stiff; contacts involving beads in the distal half use a higher v while the proximal half remains at low v.

Simulations run for $T = 0.3$ s with fine time steps.
Figure 1 shows the final 3-D configuration of the core and sleeve for unjammed and jammed simulations. In both cases, the core nodes have moved from a straight line to a gently bent shape. The beads, however, exhibit noticeably different distributions:
In the unjammed case, beads remain relatively close to the core and to each other.
In the jammed case, stronger repulsive contacts push beads further outward, producing a more diffuse bead cloud.
Figure 2 presents 3-D core centerline snapshots several times for unjammed and jammed runs. The unjammed centerlines

show more pronounced lateral excursions and irregular shapes during the transient phase, whereas the jammed centerlines remain “tighter” and closer to the x-axis. This indicates that jamming suppresses small-scale bending fluctuations and constrains the rod to move more like a stiff body.

C. Tip vertical displacement vs time

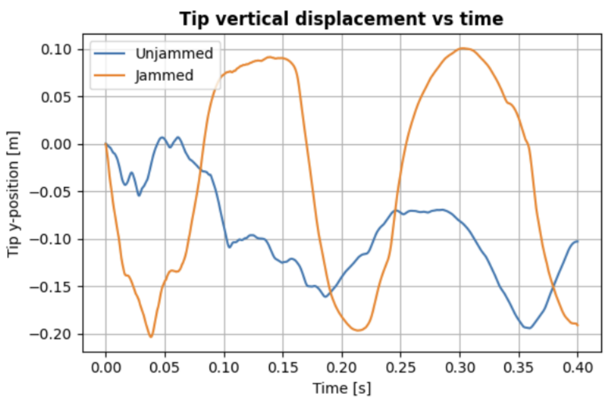

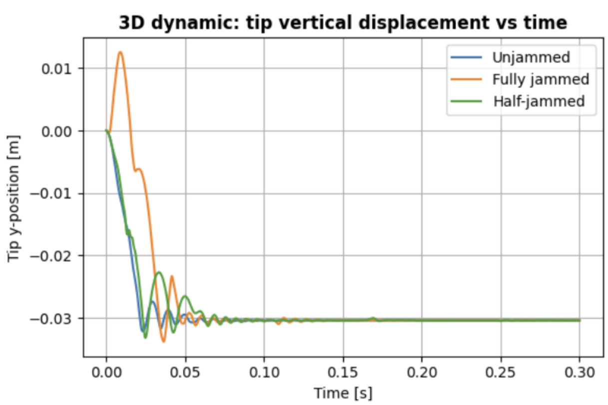

Figures plot the tip y-position versus time for the 2/3-D cases: unjammed, fully jammed, and half-jammed. All trajectories start at zero and quickly drop to around -3×10^{-2} m. The early oscillations differ slightly between cases—fully jammed shows a modest overshoot above zero before settling, and the half-jammed case has intermediate behavior—but after approximately 0.1 s all three converge to nearly identical steady values.
These results suggest that, with the present parameter choices, the steady-state tip sag is dominated by the core’s own stiffness, and the granular sleeve primarily affects transient dynamics rather than the final equilibrium position. This is in contrast to the 2-D case, where jamming significantly altered the tip deflection.

D. Curvature and Bond Energy

Figure shows the curvature along the core at the final time for unjammed, fully jammed, and half-jammed 3-D simulations. The unjammed curve exhibits high peaks, exceeding 200m^-1in localized regions, indicating sharp bends. The fully jammed curve generally has lower curvature, with peaks spread more evenly along the length. The half-jammed curve features pronounced peaks near the soft–stiff transition region, demonstrating that curvature is preferentially concentrated in the softer portion of the rod.

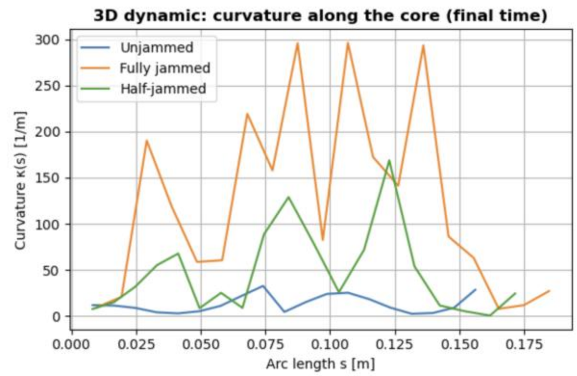

The corresponding bond energies are:

$E_{\text{bond}}^{\text{unjam}} \approx 2.5\times10^{-1}$ J, $E_{\text{bond}}^{\text{jam}} \approx 5.5\times10^{-1}$ J, $E_{\text{bond}}^{\text{half}} \approx 2.9\times10^{-1}$ J.

Thus, jammed and half-jammed cases store approximately two orders of magnitude more elastic energy in the core than the unjammed case, consistent with higher effective stiffness. The half-jammed energy lies between the two extremes, reflecting a hybrid stiffness.

E. *Dynamic 3D Vacuum Sweep*

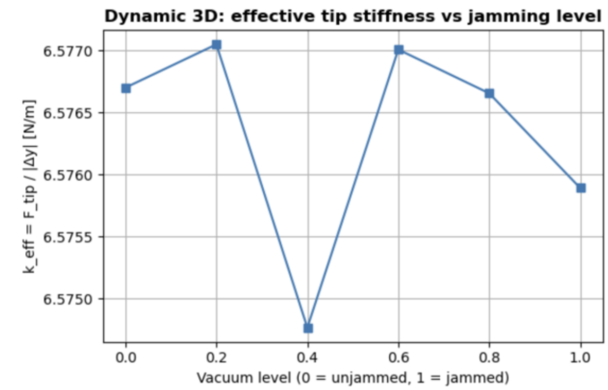

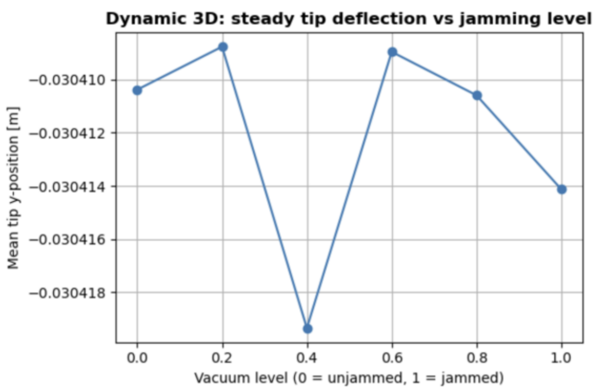

The vacuum sweep results are summarized above. The mean tip y-position varies only slightly with vacuum level, on the order of 10^{-5} m, and no clear monotonic trend appears. The effective stiffness k_{eff}also remains nearly constant, with minor non-monotone variations attributable to numerical noise and random bead packing.

These findings reinforce the conclusion from Section VI-C: for the chosen parameter regime, the elastic core dominates steady-state behavior, and adjusting uniform jamming largely affects local grain dynamics and short-time transients rather than the final tip sag.

VI. Conclusion

This project introduces a discrete element / DER-style simulation of a soft robotic segment with a granular jamming sleeve. By representing the core as a bonded particle chain and the sleeve as a collection of frictional beads whose contact stiffness is controlled by a vacuum parameter, I explore how jamming affects tip deflection, curvature, and elastic energy.
Key findings are:

- Granular jamming significantly modifies the dynamic response and curvature distribution of the segment.
- In 2-D, jamming yields large reductions in tip deflection, whereas in 3-D with current parameters it has limited impact on steady-state sag.
- Half-jammed configurations demonstrate how spatially varying jamming can control where the segment bends, concentrating curvature in soft sections.
- A Newton-based quasi-static formulation for the core is established but not yet convergent, highlighting the need for better numerical treatment.

References

[1] E. Brown *et al.*, “Universal robotic gripper based on the jamming of granular material,” *Proc. Natl. Acad. Sci. USA*, vol. 107, no. 44, pp. 18809–18814, 2010.
[2] J. Amend *et al.*, “Soft robotics commercialization: Jamming grippers from research to product,” *Soft Robotics*, vol. 3, no. 4, pp. 213–222, 2016.
[3] P. A. Cundall and O. D. L. Strack, “A discrete numerical model for granular assemblies,” *Geotechnique*, vol. 29, no. 1, pp. 47–65, 1979.
[4] Y. Hu *et al.*, “ChainQueen: A real-time differentiable physical simulator for soft robotics,” in *Proc. IEEE Int. Conf. Robotics and Automation (ICRA)*, 2019, pp. 1–7.
[5] A. Jiang *et al.*, “Design of a variable stiffness flexible manipulator with composite granular jamming and membrane coupling,” in *Proc. IEEE/RSJ Int. Conf. Intelligent Robots and Systems (IROS)*, 2012, pp. 2928–2933.
[6] W. Park *et al.*, “A hybrid jamming structure combining granules and layers for variable stiffness in soft robots,” *Soft Robotics*, vol. 9, no. 1, pp. 1–13, 2022.
[7] P. Bartkowski *et al.*, “Granular jamming for soft robotics: Experiments and modeling,” *Robotica*, 2025, in press.